New Enzyme-Activated Solubility-Switchable Contrast Agent for Magnetic Resonance Imaging: From Synthesis to in Vivo Imaging

Beata Jastrzębska,[†,‡] Réjean Lebel,[†,‡] Hélène Therriault,[‡,#] J. Oliver McIntyre,[§] Emanuel Escher,[||] Brigitte Guérin,[†,‡] Benoit Paquette,[‡,#] Witold A. Neugebauer,[||] and Martin Lepage*[,†,‡]

Centre d'Imagerie Moléculaire de Sherbrooke and Department of Nuclear Medicine and Radiobiology, Université de Sherbrooke, 3001 12e Avenue Nord, Sherbrooke, Québec J1H 5N4, Canada

Received November 7, 2008

We designed and synthesized a novel contrast agent (CA) to image the activity of matrix metalloproteinase-2 (MMP-2) in a tumor, noninvasively using magnetic resonance imaging (MRI). We exploited the concept of solubility-switchable CAs in the design of a protease-modulated CA (PCA), referred to as PCA2-switch. This PCA contains a paramagnetic gadolinium chelate (Gd-DOTA), which was attached to the N-terminus of a MMP-2 cleavable peptide sequence via a hydrophobic chain. The aqueous solubility of the CA depends on the presence of a polyethylene glycol chain (PEG) on the C-terminus of the peptide. Upon proteolytic cleavage of the peptide by MMP-2, the PEG chain is detached from the CA, which becomes less water soluble. This compound and control compounds were successfully tested in an animal model bearing two tumors with different levels of MMP-2 activity.

Introduction

The matrix metalloproteinases (MMPs) belong to a family of zinc-dependent proteinases, whose main function is the degradation of extracellular matrix components (ECM). These enzymes are present in normal healthy individuals and have a variety of functions in normal physiological conditions. However, MMPs are detected as well in pathological states in which degradation of the ECM is a key element. Their activity has been implicated in numerous disease processes including tumor cell invasion and cancer metastasis. The role of MMPs in cancer was championed by Liotta et al. who indicated that disruption of the basement membrane, a feature of invasive tumors, allows tumors to spread locally and distantly. Among over 24 members of the MMP family, MMP-2 and MMP-9 are primary effectors of these events because they hydrolyze the basal membrane type IV collagen.[1] MMP-2 has been extensively characterized, since it is an abundant protease overexpressed by many tumors. A direct correlation between MMP expression and the stage of tumor progression has been observed in various cancers including lung, breast, colon, prostate, skin, bladder, ovarian, and pancreatic cancer.[2–11] Three MMPs are frequently expressed at a high level in many human tumors: MMP-2, MMP-9, and MMP-11. For instance, in human oral squamous cell carcinomas the expression of proMMP-2 is associated with an increased frequency of lymph node metastases.[12] MMP-11 has been observed in human breast cancer tissues where its level of expression correlated with tumor progression.[4] In melanomas, the expression of MMP-9 is associated with the conversion from radial growth phase to vertical growth phase and subsequent metastasis.[7] MMP-2 is expressed on the surface of invasive tumor cells;[13] it plays a major role in the proteolysis of the basement membrane and it is associated with tumor invasion and metastasis in breast cancer.[14,15] The ability to image MMP activity is expected to be pivotal in two different areas. First, it would provide a valuable tool for detecting and measuring the activity of proteases involved in tumor invasion, potentially tailoring a treatment regimen for individual patients and for monitoring treatment response. Second, imaging MMP activity is believed to be essential in the identification and validation of anticancer targets as well as in the development of novel anticancer drugs.[16]

One of the most important diagnostic methods used to visualize soft tissues and tumors in the human body is magnetic resonance imaging (MRI). Because it does not use ionizing radiation, this imaging modality is particularly well-suited for longitudinal studies where the progression of a disease or its response to treatment can be monitored with minimal risk to the patient. Unlike optical imaging techniques that have an inherent probing depth limitation, MRI can visualize tissues throughout the human body.

Gd-DTPA (diethylenetriamine-*N*,*N*,*N*′,*N*′,*N*″-pentaacetic acid) and Gd-DOTA (1,4,7,10-tetraazacyclododecane-1,4,7,10-tetraacetic acid) were the first CAs to enter into clinical practice, and they serve as reference compounds for the development and the evaluation of new agents.[17] These low molecular weight CAs are nonspecific and are rapidly excreted by the kidneys. "Smart" contrast agents able to report on the activity of a specific enzyme have been developed.[18,19] MRI CAs are indirectly detected via their effect on the magnetic resonance longitudinal relaxation time of neighboring water molecules and the detection sensitivity is low compared with nuclear methods. A strategy to improve the effectiveness of MRI CAs has been to increase their sensitivity by incorporating large numbers of Gd(III) chelates into high molecular weight structures like polysaccharides,[20,21] poly(amino acids),[22–24] dendrimers,[25–28] and pro-

* To whom correspondence should be addressed. Address: Department of Nuclear Medicine and Radiobiology, Université de Sherbrooke, 3001 12e Avenue Nord Sherbrooke, QC J1H 5N4, Canada. Phone: 819-820-6868, extension 11867. Fax: 819-829-3238. E-mail: Martin.Lepage@USherbrooke.ca.

[†] Centre d'Imagerie Moléculaire de Sherbrooke, Université de Sherbrooke.

[‡] Department of Nuclear Medicine and Radiobiology, Université de Sherbrooke.

[#] Centre de Recherche en Radiothérapie, Université de Sherbrooke.

[§] Department of Cancer Biology and Vanderbilt-Ingram Cancer Center, Vanderbilt University, 1161 21st Avenue South, Nashville, TN 37232.

[||] Department of Pharmacology, Université de Sherbrooke, 3001 12e Avenue Nord, Sherbrooke, QC J1H 5N4, Canada.

10.1021/jm801411h CCC: $40.75
Published on Web 02/19/2009

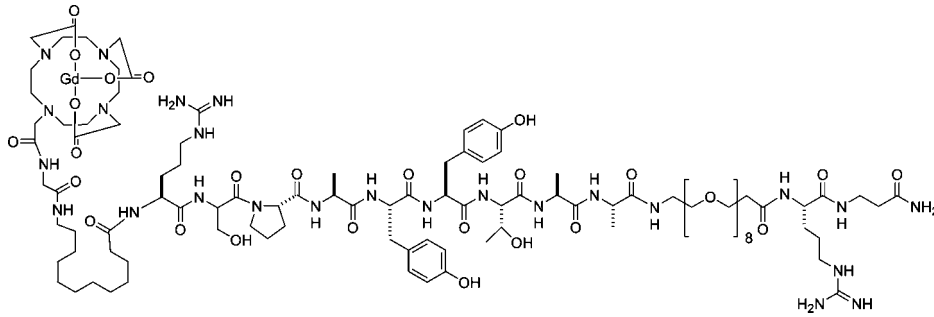

Figure 1. Sequence of PCA2-switch. The sequence SPAYYTAA, which is cleavable by MMP-2, is coupled to a PEG_8 chain and a Gd-DOTA-G-Ado conjugate.

teins.[29] Amino acids[30] and bioactive peptides[31–33] have recently been coupled to gadolinium chelates to improve MRI CA selectivity.

In the present study, we designed a novel CA agent based on a solubility switch activated by the cleavage of a peptide substrate by a specific enzyme or proteinase. This concept was recently exploited to successfully detect MMP-7.[33] Hereafter referred to as PCA2-switch, our CA is able to detect the activity of MMP-2 in a tumor implanted in a mouse in vivo and noninvasively. MMP-2 was targeted by reason of its key role in tumor progression and metastasis. A peptide has recently been reported to be cleaved efficiently and selectively by MMP-2.[34] This peptide [SGESPAY↓YTA (where "↓" indicates the cleavage site)] was chosen as the basis for the sequence of the substrate peptide of our CA, which is SPAY↓YTAA (Figure 1). A chelator of Gd was attached to the N-terminus of this peptide via a hydrophobic alkyl chain. The chelator DOTA was selected because it forms more thermodynamically and kinetically stable complexes with lanthanides, including Gd, than other chelators such as DTPA.[35,36] The hydrophobic alkyl chain (12-aminododecanoic acid, Ado) is intended to provide the desired decrease in solubility after cleavage by MMP-2 such that the cleaved CA becomes less water soluble and is retained at the tumor site.

The water solubility of the CA is dependent upon the presence of an eight-unit polyethylene glycol (PEG_8) chain at the C-terminus (Figure 1). PEG is a chemically inert synthetic polymer with unique properties such as high water solubility and low toxicity. It is widely used to improve solubility of different compounds including peptides and proteins. It has been reported that PEG conjugation can mask the surface of proteins, increases the molecular size of polypeptides, and decreases their rate of clearance from the blood circulation via intracellular uptake and kidney filtration. In addition, it modifies the biodistribution and solubility of peptides and reduces protein immunogenicity.[37–42] However, PEG conjugation may also reduce the degradation by proteolytic enzymes. On the basis of these reports, we anticipated that the introduction of PEG to the CA could be helpful to ensure a water solubility of the parent (intact or uncleaved) CA and to reduce the rate of clearance from the blood circulation. Upon cleavage of the peptide by the target MMP, the PEG chain is detached from the CA, which then becomes less water soluble and is excreted more slowly from the activation site within the tumor. There is a competition between proteolytic cleavage and the excretion of the CA; a longer circulation time will favor the cleavage event.

As a control, we synthesized a CA resistant to cleavage by MMP-2 having a scrambled sequence (SYPATAYA) of the MMP-2-cleavable peptide. This CA will hereafter be referred to as PCA2-scrambled.

Results and Discussion

Synthesis of the CAs. The novel peptide-based CA was designed to detect in vivo and noninvasively the activity of MMP-2. The design is based on a switch of solubility, whereby the water solubility of the CA is decreased after selective enzyme cleavage. The introduction of a hydrophobic moiety (a fatty acid, Ado) was the key element in reducing the solubility of the CAs after cleavage by MMP-2. To improve the yield and to facilitate DOTA-tris(*t*-Bu) coupling, a glycine residue was introduced between DOTA and Ado into the CA sequence. Some difficulties were initially observed during synthesis of our compounds (e.g., incomplete *t*-Bu esters cleavage, poor yield, weak response to Kaiser's test) as previously described in the literature.[43,44] The yield was improved by increasing the cleavage time up to 3.5 h. We also increased the ratio of scavengers such as 1,2-ethanedithiol (EDT[a]) and thioanisole (TA) from 2:3 to 4:6 before addition of the cleavage mixture ($TFA/H_2O/EDT/TA = 87.5:2.5:4:6$ v/v/v/v) and found that this minimized side reactions. Finally, after purification, high purity products were obtained (98−99%).

The CAs must be hydrophilic before injection into animals such that a very hydrophilic C-terminus was designed, including a β-alanine spacer and hydrophilic components (i.e, PEG and Arg). The expected molecular masses were found for PCA2-switch ($C_{103}H_{170}GdN_{25}O_{33}$ $[M + H]^+_{found} = 2444.78$, $[M + H]^+_{calc} = 2443.85$ (see Supporting Information Figure 1)) and PCA2-scrambled ($C_{103}H_{170}GdN_{25}O_{33}$ $[M + H]^+_{found} = 2444.79$, $[M + H]^+_{calc} = 2443.85$ (see Supporting Information Figure 2)). These data along with the corresponding HPLC elution times are reported in Table 2.

Peptide Cleavage Efficiency. The efficiency of enzymatic cleavage (k_{cat}/K_m) by MMP-2 was determined, and the results are presented in Table 1. The k_{cat}/K_m value of Ac-SGESPAYYTA (**I**) was comparable but slightly smaller than that reported by Chen et al. for this peptide (called peptide B74P).[34] This difference may be explained by the form of MMP-2 used in the assay. The enzymatic assays of Chen et al. were performed using the catalytic fragment of MMP-2 produced in their laboratory, while we used the complete enzyme. The cleavage efficiency of the peptide Ac-SPAYYTAA-NH_2 (**II**) was also

[a] Abbreviations: EDT, 1,2-ethanedithiol; HATU, 2-(1*H*-7-azabenzotriazol-1-yl)-1,1,3,3-tetramethyluronium hexafluorophosphate; PyBOP, benzotriazole-1-yloxy-tris-pyrolidinophosphonium hexafluorophasphate; TIPS, triisopropylsilane; TBTU, 2-(1*H*-benzotriazol-1-yl)-1,1,3,3-tetramethyluronium tetrafluoroborate; TFA, trifluoroacetic acid; Ado, 12-aminododecanoic acid; β-Ala, β-alanine; Ac, acetyl; *i*-Pr-OH, isopropanol; WT, wild-type; KD, knock-down.

Table 1. Enzymatic Cleavage Efficiency of Peptides

peptide number	peptide sequence	k_{cat}/K_m (M^{-1} s^{-1})
I	Ac-SGESPAYYTA-NH_2	$(16 \pm 4) \times 10^4 (44 \times 10^4)^a$
II	Ac-SPAYYTAA-NH_2	$(31 \pm 6) \times 10^4$
III	DOTA(Gd)-G-Ado-RSPAYYTAA-PEG_8-R-β-Ala-NH_2	$(12 \pm 2) \times 10^4$
IV	DOTA(Gd)-G-Ado-RSYPATAYA-PEG_8-R-β-Ala-NH_2	$(3 \pm 2) \times 10^3$

[a] k_{cat}/K_m determined by Chen et al.

Table 2. Characterization of the CAs and Their Fragments

			molecular weight[b] (Da)		
peptide number	peptide sequence	t_R[a] (min)	calculated	found	log P [c]
III	DOTA(Gd)-G-Ado-RSPAYYTAA-PEG_8-R-β-Ala-NH_2	12.6	2443.85	2444.78	<-4.18
IV	DOTA-G-Ado-RSYPATAYA-PEG_8-R-β-Ala-NH_2	12.6	2443.85	2444.79	<-4.18
A	YTAA-PEG_8-R-β-Ala-NH_2	9.9	1074.23	1074.94	<-4.18
B	DOTA(Gd)-G-Ado-RSPAY-OH	12.4	1387.64	1388.58	-2.18 ± 0.03
C	YA-PEG_8-R-β-Ala-NH_2	10.3	902.04	901.91	nd
D	AYA-PEG_8-R -β-Ala-NH_2	10.3	973.12	973.64	nd
E	DOTA(Gd)-G-Ado-RSYPAT-OH	12.2	1488.74	1488.41	nd
F	DOTA(Gd)-G-Ado-RSYPATA-OH	12.2	1559.82	1559.28	nd

[a] HPLC retention time (t_R). A linear gradient from 0% to 100% CH_3CN (0.1% TFA) in H_2O (0.1% TFA) in 30 min at a flow rate of 1 mL/min was used. [b] As found by MALDI-TOF MS. [c] Partition coefficient (log P values).

similar. The peptide is modified from peptide B74P of Chen et al. including the seven residues that correspond to P4 to P3′ and adding a C-terminal A as the P4′ residue of the octapeptide substrate that can be accommodated in the catalytic site of MMP-2.[45] Then we determined whether this peptide was still efficiently cleaved by MMP-2 after DOTA(Gd) was coupled to the G-Ado-RSPAYYTAA-PEG_8 chain (**III**). The cleavage efficiency of PCA2-switch (**III**) was $(12 \pm 2) \times 10^4$ M^{-1} s^{-1}, which is comparable with the k_{cat}/K_m of the unmodified peptide. The reaction products of the enzymatic cleavage were separated by HPLC and analyzed by mass spectrometry (see Supporting Information Figure 3). The peaks were identified as YTAA-PEG_8-R-β-Ala-NH_2 (**A**) ($[M + H]^+_{found} = 1074.94$, $[M + H]^+_{calc} = 1074.23$) and DOTA(Gd)-G-Ado-RSPAY-OH (**B**) ($[M + H]^+_{found} = 1388.58$, $[M + H]^+_{calc} = 1387.64$), whereas the parent compound was not detected.

The efficiency of enzymatic cleavage of PCA2-scrambled (**IV**) incorporating the scrambled peptide sequence (SYPATAYA) was 37.5 times lower (3.2×10^3 M^{-1} s^{-1}) than the nonscrambled analogue **III** ($(12 \pm 2) \times 10^4$ M^{-1} s^{-1}). The parent compound **IV** was still detected after incubation with MMP-2 (see Supporting Information Figure 4), although degradation products were also observed (see Supporting Information Figure 4). Two pairs of products were identified as YA-PEG_8-R-β-Ala-NH_2 (**C**) ($[M + H]^+_{found} = 901.91$, $[M + H]^+_{calc} = 902.04$), AYA-$PEG_8$-R-$\beta$-Ala-$NH_2$ (**D**) ($[M + H]^+_{found} = 973.64$, $[M + H]^+_{calc} = 973.12$), DOTA(Gd)-G-Ado-RSYPAT-OH (**E**) ($[M + H]^+_{found} = 1488.41$, $[M + H]^+_{calc} = 1488.74$), DOTA(Gd)-G-Ado-RSYPATA-OH (**F**) ($[M + H]^+_{found} = 1559.28$, $[M + H]^+_{calc} = 1559.82$) by mass spectrometry (Table 2). These results indicate that the peptide substrate of the PCA2-switch is efficiently cleaved by MMP-2 in the expected position. In contrast, the peptide substrate of PCA2-scrambled was not efficiently or specifically cleaved.

In Vitro Observation of the Solubility Switch. The relative amount of a compound dissolved in octanol and in water was determined using HPLC. Intact PCA2-switch, **III**, and PCA2-scrambled, **IV**, are highly water soluble as judged from their log P values, which were below our measurement uncertainty (i.e., $\log P \leq -4.18$) because an HPLC signal in the octanol phase could not be detected. The cleavage product bearing the Gd chelate [DOTA(Gd)-G-Ado-RSPAY-OH, **B**] was less water soluble with $\log P = -2.18 \pm 0.03$. These values are in accordance with predictions of -5.74 and -1.61 calculated from the Molinspiration Cheminformatics online tool.[46] This clearly illustrates the decrease in solubility upon cleavage of PCA2-switch.

In Vivo Testing of CAs. The ability of PCA2-switch to detect the activity of MMP-2 was tested on an animal model with two tumors, one grown from MC7-L1-WT cells that overexpress MMP-2 compared to normal tissues and the other tumor grown from MC7-L1-KD cells, having a MMP-2 activity reduced by ~50%.

MRI results obtained for PCA2-switch, PCA2-scrambled, and Gd-DTPA (Magnevist, Berlex) injected into animals within the MRI scanner were reported elsewhere.[47] Briefly, an immediate signal increase was observed in the two tumors for the three agents, and this is attributed to the blood perfusion of the tumors. The increase of longitudinal relaxivity (ΔR_1) was normalized to this early maximum to control for tumor-to-tumor variations in blood perfusion. After injection of PCA2-switch, the relative ΔR_1 value reached a temporary plateau in the MC7-L1-WT tumors between 5 and 10 min after injection. This was followed by a large maximum at around 40 min after injection, whereas only a continuous decrease is observed in the MC7-L1-KD tumors. After injection of PCA2-scrambled, the early maximum was immediately followed by a continuous decrease. An additional control using Gd-DTPA revealed a similar kinetics for the MC7-L1-WT and MC7-L1-KD both tumors, indicating that vascular permeability is comparable for both tumors. A large signal intensity increase was observed by MRI in the bladder of animals, which suggested elimination of the CA via the urinary system. Our interpretation was that cleavage of PCA2-switch in the MC7-L1-WT tumor resulted in an accumulation of the cleaved PCA2-switch. This confirmed that the solubility switch approach is effective in vivo.

In summary, the method for preparation of a novel peptide-based CA and its in vivo performance are demonstrated. This compound could provide a unique tool in the noninvasive tumor phenotyping and guide in the treatment planning for individual cancer patients. The potential for this agent to monitor the activity of MMP-2 as a function of treatment response or as a biomarker of tumor aggressiveness will be investigated.

Experimental Procedures

Materials. All chemicals and solvents were purchased from commercial sources and were used without further purification. Analytical high performance liquid chromatography (HPLC) was

performed on an Agilent 1100 system equipped with a Agilent 1100 series diode array UV/vis detector and a Zorbax Eclipse XDB C_{18} reverse phase column (4.6 mm × 250 mm, 5 μm). A linear gradient from 0% to 100% CH_3CN (0.1% TFA) in H_2O (0.1% TFA) in 30 min at a flow rate of 1 mL/min was used for peptide conjugates (20−60% for acetylated peptides).

Semipreparative HPLC was conducted on a Agilent 1100 instrument equipped with a Agilent 1100 series diode array UV/vis detector on a Zorbax Eclipse XDB C_{18} reverse phase column (9.4 mm × 250 mm, 5 μm). Acetylated peptides were eluted using a linear gradient (10 −100%) of CH_3CN/0.1% TFA in H_2O/0.1% TFA at a flow rate of 2 mL/min in 40 min.

Preparative scale chromatography was carried out using C_{18} glass column at medium pressure. A linear gradient (0−100%) of CH_3CN/0.1%TFA in H_2O/0.1% TFA was used, and the separation was monitored at 254 nm.

The purity of compounds was determined by the ratio of the integrated HPLC peak area for the compound of interest over the integrated HPLC peak area for all peaks. For every molecule synthesized, the purity was >95%.

Matrix assisted laser desorption ionization time-of-flight mass spectrometry (MALDI-TOF MS) analyses were recorded on a Micromass TofSpec 2E instrument. Measurements were made in the linear mode with α-cyano-4-hydroxycinnamic acid as the matrix.

Solid Phase Peptide Synthesis. Solid phase peptide synthesis was carried out following Fmoc strategy using TentaGel S RAM resin (in the form of Rink amide). Peptides with the following sequences DOTA-G-Ado-RSPAYYTAA-PEG_8-R-β-Ala-NH_2 and DOTA-G-Ado-RSYPATAYA-PEG_8-R-β-Ala-NH_2 were synthesized manually using single step couplings with 2-fold excess of Fmoc-amino acids, 2-fold excess of TBTU as activating reagent, and 4-fold excess of *N*,*N*-diisopropylethylamine (DIPEA) in *N*,*N*-dimethylformamide (DMF) for 2 h at room temperature. Fmoc-amido-PEG_8-OH was coupled to PyBOP/DIPEA (1:2) in dichloromethane (DCM) and Fmoc-12-Ado-OH with HATU/DIPEA (1:2) in DMF. Fmoc-AAs were preactivated for 2 min prior to coupling. The terminal amino groups were deprotected with 20% piperidine in DMF (1 × 10 min and 1 × 20 min). Deprotection and coupling steps were followed by Kaiser's test.[48] After each step the peptide resins were washed with DMF (1×), DCM (3×), DCM/*i*-Pr-OH (3×), *i*-Pr-OH (3×), and DCM (3×). Peptides with the following sequences Ac-SPAYYTAA-NH_2 and Ac-SGES-PAYYTA-NH_2 were synthesized on a continuous flow peptide synthesis system (Pioneer) using standard Fmoc protocols with TBTU couplings. The final N-acetylation was carried out using of 20% acetic anhydride in DCM in the presence of DIPEA for 1 h at room temperature. The peptide resins were washed with DCM (3×), DCM/*i*-Pr-OH (3×), *i*-Pr-OH (3×), and DCM (3×).

Acetylated peptides were deprotected and cleaved from the polymer support by addition of TFA/H_2O/TIPS (95:2.5:2.5, v/v/v) for 1 h at room temperature. The resin was removed by filtration and washed with TFA. Combined filtrates were added dropwise to ethyl ether. The precipitated peptides were centrifuged, dissolved in 20% CH_3CN/H_2O, frozen, and lyophilized. The crude products were purified by semipreparative HPLC. The purity of peptides was verified by analytical HPLC, and their identity was confirmed with MALDI mass spectrometry.

The final cleavage of the DOTA−peptide conjugates from the resin together with the removal of the side chain protecting groups were carried out with TFA/H_2O/EDT/TA (87.5:2.5:4:6, v/v/v/v), where EDT/TA was added first, for 3.5 h at room temperature. The cleavage mixture was filtered and the resin rinsed with neat TFA. The filtrates were added dropwise to ethyl ether. The precipitates were centrifuged, dissolved in 20% CH_3CN/H_2O, frozen, and lyophilized. The crude products were purified on preparative C_{18} glass chromatography column at medium pressure. The purified peptides were analyzed by analytical HPLC and mass spectrometry.

Preparation of Gd Complexes. The DOTA−peptides were dissolved in deionized water, and pH was adjusted to 6−7 by adding 0.3% NH_4OH (aq). An amount of 2 equiv of gadolinium chloride hexahydrate in 1 mL water was added, and pH was kept stable. The reaction mixtures were vigorously stirred for 24 h, frozen, and lyophilized. The complexes were purified by preparative chromatography as described above. The appropriate fractions were pooled, lyophilized, and characterized by analytical HPLC, and their identity was confirmed by MALDI-TOF spectrometry.

Partition Coefficients. The hydrophilic/hydrophobic properties of the compounds were determined by their partition coefficient (log *P*) between *n*-octanol/water. The integrated signal at 240 nm using a standard volume of sample from both phases in analytical HPLC was measured. The log *P* value was calculated by taking the logarithm of the integral in *n*-octanol divided by that from PBS. Experiments were performed in triplicate, and results are presented as the mean value and the standard deviation from the mean.

Peptide Cleavage by MMP-2. The affinity (K_m) and the efficacy of enzymatic cleavage (k_{cat}/K_m) of the peptide sequence were determined. The enzymatic assay was based on the detection by fluorescamine of the free amino group on the cleaved peptide sequence of the compounds.[49] Background signal from free amines was subtracted from the fluorescence signal variations recorded after addition of the enzyme. This assay was adapted to a 96-well plate from a published methodology,[50] and the K_m and k_{cat}/K_m were determined according to the protocol proposed by Fields et al.[51]

The K_m values were determined by incubating the compounds at a concentration ranging from 0 to 40 μM with 40 nM MMP-2 in tricine buffer (50 mM tricine, pH 7.5, 50 mM NaCl, 10 mM $CaCl_2$, 0.05% Brij-35) at 37 °C. The rate of hydrolysis (v) was determined by measuring the amount of CA cleaved after 30 s for each CA concentration. At the appropriate time interval, 20 μL aliquots of the incubation solution were withdrawn and added to 30 μL of 20 mM 1,10-phenanthroline to stop the reaction. A stock solution of 1,10-phenanthroline at 0.5 M was prepared in DMSO and diluted to 20 mM in tricine buffer immediately before use. In a 96-well assay plate, the incubation solution was mixed with 200 μL of fluorescamine at 5 mM. Relative fluorescence units (RFU) were measured using a 96-well plate reader Synergy HT (BIOTEK Instruments, Winooski, VT) set at a λ_{ex} = 400 nm and a λ_{em} = 460 nm. K_m was calculated according to the Eadie−Hoffstee method by plotting the enzymatic rate v (in relative fluorescence units, RFU/s) vs v/[CA], where the resulting slope is equal to $-K_m$.

The values of k_{cat}/K_m were determined by mixing the CA at a fixed concentration of 10 μM with 40 nM MMP-2 in tricine buffer at 37 °C. The reaction was stopped at 0.5, 1, 2, 3, 4, 6.5, and 10 min for PCA2-switch and at 0.5, 1, 2, 4, 6, and 24 h for PCA2-scrambled by mixing 20 μL aliquots of the incubation solution with 30 μL of 20 mM 1,10-phenanthroline as previously described. Fluorescamine was added and the fluorescence measured. The initial rate (v_i) was calculated from values of less than 40% of CA hydrolysis by plotting the fluorescence of each sample as a function of the incubation time. The units were converted to v_i = [slope (RFU/s)][CA (M)]/(Δ RFU) at 100% hydrolysis. The units of v_i and concentrations were M/s and M, respectively. The k_{cat}/K_m values were calculated using the following expression:

$$\frac{k_{cat}}{K_m} = \frac{v_i}{[CA][MMP\text{-}2]}$$

The cleavage products were identified by analytical HPLC and collected and their masses determined using mass spectrometry.

Mouse Model. The CAs were tested on the MC7-L1 mammary carcinoma mouse model. Balb/c mice were injected subcutaneously in the left hind limb with 1 × 10^7 MC7-L1 cells knocked down (MC7-L1-KD) for MMP-2 as published elsewhere.[47] One week later 2 × 10^6 wild-type MC7-L1 (MC7-L1-WT) cells were injected subcutaneously in the right hind limb. The timing and the number of cells accounted for the more rapid growth of WT cells. After 4 weeks, the average volumes for 4 animals were 235 ± 195 mm^3 for the MC7-L1-WT tumors and 215 ± 102 mm^3 for the MC7-L1-KD tumors. The difference was not significant. The activity of MMP-2 in MC7-L1-KD tumors was reduced by 50% compared with MC7-L1-KD cells.[47]

Acknowledgment. E.E., W.A.N., B.P., and M.L. are members of the FRSQ-funded Centre de Recherche Clinique Étienne-LeBel. M.L. is the Canada Research Chair in magnetic resonance imaging. We acknowledge the help of M. Archambault, C. Dubuc, and V. Dumulon-Perreault. Partial funding from CIHR (Grant No. NTA71855) is acknowledged. This work was supported by the National Cancer Institute of Canada (Grant No. 016436).

Supporting Information Available: HPLC and MALDI-TOF MS spectra of PCA2-switch and PCA2-scrambled before and after treatment with MMP-2. This material is available free of charge via the Internet at http://pubs.acs.org.

References

(1) Liotta, L. A.; Tryggvason, K.; Garbisa, S.; Hart, I.; Foltz, C. M.; Shafie, S. Metastatic potential correlates with enzymatic degradation of basement membrane collagen. *Nature* **1980**, *284*, 67–68.
(2) Urbanski, S. J.; Edwards, D. R.; Maitland, A.; Leco, K. J.; Watson, A.; Kossakowska, A. E. Expression of metalloproteinases and their inhibitors in primary pulmonary carcinomas. *Br. J. Cancer* **1992**, *66*, 1188–1194.
(3) Remacle, A. G.; Noël, A.; Duggan, C.; McDermott, E.; O'Higgins, N.; Foidart, J. M.; Duffy, M. Assay of matrix metalloproteinases types 1, 2, 3, and in breast cancer. *Br. J. Cancer* **1998**, *77*, 926–931.
(4) Basset, P.; Bellocq, J. P.; Wolf, C.; Stoll, I.; Hutin, P.; Limacher, J. M.; Podhajcer, O. L.; Chenard, M. P.; Rio, M. C.; Chambon, P. A novel metalloproteinase gene specifically expressed in stromal cells of breast carcinomas. *Nature* **1990**, *348*, 699–704.
(5) Parsons, S. L.; Watson, S. A.; Collins, H. M.; Griffin, N. R.; Clarke, P. A.; Steele, R. J. C. Gelatinase (MMP-2 and -9) expression in gastrointestinal malignancy. *Br. J. Cancer* **1998**, *78*, 1495–1502.
(6) Stearns, M. E.; Wang, M. Type IV collagenase (M_r 72,000) expression in human prostate: Bening and malignant tissue. *Cancer Res.* **1993**, *53*, 878–883.
(7) MacDougall, J. R.; Bani, M. R.; Lin, Y.; Rak, J.; Kerbel, R. S. The 92-kDa gelatinase B is expressed by advanced stage melanoma cells: suppression by somatic cell hybridization with early stage melanoma cell. *Cancer Res.* **1995**, *55*, 4174–4181.
(8) Gerhards, S.; Jung, K.; Koenig, F.; Daniltchenko, D.; Hauptmann, S.; Schnorr, D.; Loening, S. A. Excretion of matrix metalloproteinases 2 and 9 in urine is associated with a high stage and grade of bladder carcinoma. *Urology* **2001**, *57*, 675–679.
(9) Schmalfeldt, B.; Prechtel, D.; Härting, K.; Späthe, K.; Rutke, S.; Konik, E.; Fridman, R.; Berger, U.; Schmitt, M.; Kuhn, W.; Lengyel, E. Increased expression of matrix metalloproteinases (MMP)-2, MMP-9, and the urokinase-type plasminogen activator is associated with progression from benign to advanced ovarian cancer. *Clin. Cancer Res.* **2001**, *7*, 2396–2404.
(10) Koshiba, T.; Hosotani, R.; Wada, M.; Fujimoto, K.; Lee, J.; Doi, R.; Arii, S.; Imamura, M. Detection of matrix metalloproteinase activity in human pancreatic cancer. *Surg. Today* **1997**, *27*, 302–304.
(11) Langers, A. M. J.; Sier, C. F. M.; Hawinkels, L. J. A. C.; Kubben, F. J. G. M.; van Duijn, W.; van der Reijden, J. J.; Lamers, C. B. H. W.; Hommes, D. W.; Verspaget, H. W. MMP-2 geno-phenotype is prognostic for colorectal cancer survival, whereas MMP-9 is not. *Br. J. Cancer* **2008**, *98*, 1820–1823.
(12) Kusukawa, J.; Sasaquri, Y.; Shima, I.; Kameyama, T.; Morimatsu, M. Expression of matrix metalloproteinase-2 releated to lymph node metastasis of oral squamous cell carcinoma. A clinicopathologic study. *Am. J. Clin. Pathol.* **1993**, *99*, 18–23.
(13) Sato, H.; Takino, T.; Okada, Y.; Cao, J.; Shinagawa, A.; Yamamoto, E.; Selki, M. A matrix metalloproteinase expressed on the surface of invasive tumour cells. *Nature* **1994**, *370*, 61–65.
(14) Gilles, C.; Bassuk, J. A.; Pulyaeva, J.; Sage, E. H.; Foidart, J. M.; Thompson, E. W. SPARC/osteonectin induces matrix metalloproteinase-2 activation in human breast cancer cell lines. *Cancer Res.* **1998**, *58*, 5529–5536.
(15) Jones, J. L.; Glynn, P.; Walker, R. A. Expression of MMP-2 and MMP-9, their inhibitors and the activator MT1-MMP in primary breast carcinomas. *J. Pathol.* **1999**, *189*, 161–168.
(16) Overall, C. M.; Kleifeld, O. Validating matrix metalloproteinases as drug targets and anti-targets for cancer therapy. *Nat. Rev. Cancer* **2006**, *6*, 227–239.
(17) Bellin, M. F.; Vasile, M.; Morel-Precetti, S. Currently used non-specific extracellular MR contrast media. *Eur. Radiol.* **2003**, *13*, 2688–2698.
(18) Moats, R. A.; Fraser, S. E.; Meade, T. J. A "smart" magnetic resonance imaging agent that reports on specific enzymatic activity. *Angew. Chem., Int. Ed. Engl.* **1997**, *36*, 726–728.
(19) Louie, A. Y.; Hüber, M. M.; Ahrens, E. T.; Rothbächer, U.; Moats, R.; Jacobs, R. E.; Fraser, S. E.; Meade, T. J. In vivo visualization of gene expression using magnetic resonance imaging. *Nat. Biotechnol.* **2000**, *18*, 321–325.
(20) Armitage, F. E.; Richardson, D. E.; Li, K. C. P. Polymeric contrast agent for magnetic resonance imaging: synthesis and characterization of gadolinium diethylenetriaminepentaacetic acid conjugated to polysaccharides. *Bioconjugate Chem.* **1990**, *1*, 365–374.
(21) André, J. P.; Geraldes, C. F. G. C.; Martins, J. A.; Merbach, A. E.; Prata, M. I. M.; Santos, A. C.; de Lima, J. J. P.; Tóth, É. Lanthanide(III) complexes of DOTA−glycoconjugates: a potential new class of lectin-mediated medical imaging agents. *Chem.—Eur. J.* **2004**, *10*, 5804–5816.
(22) Weissleder, R.; Bogdanov, A.; Tung, C. H.; Weinmann, H. J. Size optimization of synthetic graft copolymers for in vivo angiogenesis imaging. *Bioconjugate Chem.* **2001**, *12*, 213–219.
(23) Lu, Z. R.; Wang, X. H.; Parker, D. L.; Goodrich, K. C.; Buswell, H. R. Poly(L-glutamic acid) Gd(III)−DOTA conjugate with a degradable spacer for magnetic resonance imaging. *Bioconjugate Chem.* **2003**, *14*, 715–719.
(24) Lee, H. Y.; Jee, H. W.; Seo, S. M.; Kwak, B. K.; Khang, G.; Cho, S. H. Diethylenetriaminepentaacetic acid-gadolinium (DTPA-Gd)-conjugated polysuccinimide derivatives as magnetic resonance imaging contrast agents. *Bioconjugate Chem.* **2006**, *17*, 700–706.
(25) Wiener, E. C.; Brechbiel, M. W.; Brothers, H.; Magin, R. L.; Gansow, O. A.; Tomalia, D. A.; Lauterbur, P. C. Dendrimer-based metal chelates, a new class of magnetic resonance imaging contrast agents. *Magn. Reson. Med.* **1994**, *31*, 1–8.
(26) Wiener, E. C.; Konda, S.; Shadron, A.; Brechbiel, M.; Gansow, O. Targeting dendrimer-chelates to tumors and tumor cells expressing the high-affinity folate receptor. *Invest. Radiol.* **1997**, *32*, 748–754.
(27) Kobayashi, H.; Kawamoto, S.; Saga, T.; Sato, N.; Hiraga, A.; Ishimori, T.; Konishi, J.; Togashi, K.; Brechbiel, M. W. Positive effects of polyethylene glycol conjugation to generation-4 polyamidoamine dendrimers as macromolecular MR contrast agents. *Magn. Reson. Med.* **2001**, *46*, 781–788.
(28) Kobayashi, H.; Kawamoto, S.; Star, R. A.; Waldmann, T. A.; Tagaya, Y.; Brechbiel, M. W. Micro-magnetic resonance lymphangiography in mice using a novel dendrimer-based magnetic resonance imaging contrast agent. *Cancer Res.* **2003**, *63*, 271–276.
(29) Schmiedl, U.; Ogan, M.; Paajanen, H.; Marotti, M.; Crooks, L. E.; Brito, A. C.; Brasch, R. C. Albumin labeled with Gd-DTPA as an intravascular, blood pool-enhancing agent for MR imaging: biodistribution and imaging studies. *Radiology* **1987**, *162*, 205–210.
(30) Geninatti Crich, S.; Cabella, C.; Barge, A.; Belfiore, S.; Ghirelli, C.; Lattuada, L.; Lanzardo, S.; Mortillaro, A.; Tei, L.; Visigalli, M.; Forni, G.; Aime, S. In vitro and in vivo magnetic resonance detection of tumor cells by targeting glutamine transporters with Gd-based probes. *J. Med. Chem.* **2006**, *49*, 4926–4936.
(31) Dirksen, A.; Langereis, S.; de Waal, B. F. M.; van Genderen, M. H. P.; Meijer, E. W.; de Lussanet, Q. G.; Hackeng, T. M. Design and synthesis of a bimodal target-specific contrast agent for angiogenesis. *Org. Lett.* **2004**, *6*, 4857–4860.
(32) Bull, S. R.; Guler, M. O.; Bras, R. E.; Meade, T. J.; Stupp, S. I. Self-assembled peptide amphiphile nanofibers conjugated to MRI contrast agents. *Nano Lett.* **2005**, *5*, 1–4.
(33) Lepage, M.; Dow, W. C.; Melchior, M.; You, Y.; Fingleton, B.; Quarles, C. C.; Pépin, C.; Gore, J. C.; Matrisian, L. M.; McIntyre, J. O. Non-invasive detection of matrix metalloproteinase activity in vivo using a novel MRI contrast agent with a solubility switch. *Mol. Imaging* **2007**, *6*, 393–403.
(34) Chen, E. I.; Kridel, S. J.; Howard, E. W.; Li, W.; Godzik, A.; Smith, J. W. A unique substrate recognition profile for matrix metalloproteinase-2. *J. Biol. Chem.* **2002**, *277*, 4485–4491.
(35) Loncin, M. F.; Desreux, J. F.; Merciny, E. Coordination of lanthanides by 2 polyamino polycarboxylic macrocycles: formation of highly stable lanthanide complexes. *Inorg. Chem.* **1986**, *25*, 2646–2648.
(36) Aime, S.; Botta, M.; Fasano, M.; Terreno, E. Lanthanide(III) chelates for NMR biomedical applications. *Chem. Soc. Rev.* **1998**, *27*, 19–29.
(37) DeNardo, S. J.; Yao, Z. S.; Lam, K. S.; Song, A. M.; Burke, P. A.; Mirick, G. R.; Lamborn, K. R.; O'Donnel, L. R. T.; DeNardo, G. L. Effect of molecular size of pegylated peptide on the pharmacokinetics and tumor targeting in lymphoma-bearing mice. *Clin. Cancer Res.* **2003**, *9*, 3854s–3864s.
(38) Hershfield, M. PEG-ADA replacement therapy for adenosine deaminase deficiency: an update after 8.5 years. *Clin. Immunol. Immunopathol.* **1995**, *76*, S228–S232.
(39) Abuchowski, A.; McCoy, J. R.; Palczuk, N. C.; van Es, T.; Davis, F. F. Effect of covalent attachment of polyethylene glycol on immunogenicity and circulating life of bovine liver catalase. *J. Biol. Chem.* **1977**, *252*, 3582–3587.

(40) Bukowski, R. M.; Tendler, C.; Cutler, D.; Rose, E.; Laughlin, M. M.; Statkevich, P. Treating cancer with PEG intron. Pharmacokinetic profile and dosing guidelines for an improved interferon-alpha-2b formulation. *Cancer* **2002**, *95*, 389–396.
(41) Wilkinson, J.; Jackson, C. J. C.; Lang, G. M.; Holford-Strevens, V.; Sehon, A. H. Tolerance induction in mice by conjugates of monoclonal immunoglobulins and monomethoxypolyethylene glycol. Transfer of tolerance by T-cells and by T-cells extracts. *J. Immunol.* **1987**, *139*, 326–331.
(42) Tsutsumi, Y.; Onda, M.; Nagata, S.; Lee, B.; Kreitman, R. J.; Pastan, I. Site-specific chemical modification with polyethylene glycol of recombinant immunotoxin anti-Tac(Fv)-PE38 (LMB-2) improves antitumor activity and reduces animal toxicity and immunogenicity. *Proc. Natl. Acad. Sci. U.S.A.* **2000**, *97*, 8548–8553.
(43) Schottelius, M.; Schwaiger, M.; Wester, H.-J. Rapid and high-yield solution-phase synthesis of DOTA-Tyr3-octreotide and DOTA-Tyr3-octreotate using unprotected DOTA. *Tetrahedron Lett.* **2003**, *44*, 2393–2396.
(44) Chen, X. Y.; Park, R.; Hou, Y. P.; Tohme, M.; Shahinian, A. H.; Bading, J. R.; Conti, P. S. MicroPET and autoradiographic imaging of GRP receptor expression with ^{64}Cu-DOTa-[Lys^{3}]bombesin in human prostate adenocarcinoma xenografts. *J. Nucl. Med.* **2004**, *45*, 1390–1397.
(45) Woessner, J. F.; Nagase, H. *Matrix Metalloproteinases and TIMPs*; Oxford University Press: Oxford, U.K., 2000.
(46) Molinspiration Cheminformatics Calculation of Molecular Properties and Drug-likeness. http://www.molinspiration.com (accessed April 2008).
(47) Lebel, R.; Jastrzębska, B.; Therriault, H.; Cournoyer, M.-M.; McIntyre, J. O.; Neugebauer, W.; Escher, E.; Paquette, B.; Lepage, M. Novel solubility-switchable MRI agent allows the noninvasive detection of matrix metalloproteinase-2 activity activity in vivo in a mouse model. *Magn. Reson. Med.* **2008**, *60*, 1056–1065.
(48) Kaiser, E.; Colescott, R. L.; Bossinger, C. D.; Cook, P. I. Color test for detection of free terminal amino groups in the solid-phase synthesis of peptides. *Anal. Biochem.* **1970**, *34*, 595–598.
(49) Udenfriend, S.; Stein, S.; Böhlen, P.; Dairman, W.; Leimgruber, W.; Weigele, M. Fluorescamine: a reagent for assay of amino acids, peptides, proteins, and primary amines in the picomole range. *Science* **1972**, *178*, 871–872.
(50) Lauer-Fields, J. L.; Sritharan, T.; Stack, M. S.; Nagase, H.; Fields, G. B. Selective hydrolysis of triple-helical substrates by matrix metalloproteinase-2 and -9. *J. Biol. Chem.* **2003**, *278*, 18140–18145.
(51) Fields, G. B.; Van Wart, H. E.; Birkedal-Hansen, H. Sequence specificity of human skin fibroblast collagenase. Evidence for the role of collagen structure in determining the collagenase cleavage site. *J. Biol. Chem.* **1987**, *262*, 6221–6226.

JM801411H